MONITOR PROPORTIONAL COUNTER

M. C. Weisskopf
NASA, Marshall Space Flight Center

INTRODUCTION

One of the instruments on the HEAO-2/Einstein Observatory is the Monitor Proportional Counter (MPC). The MPC and its associated electronics have been described in detail elsewhere (Gaillardetz et al., 1978 and Giacconi et al., 1979) and will only be reviewed briefly here. The MPC is an Uhuru class Ar-CO_2 gas-filled proportional counter sealed with a 1.5 mil beryllium window and sensitive to X-rays in the energy bandwidth from 1.5 to 22 keV. Both pulse shape discrimination and anticoincidence cells are used to limit the background counting rate to 20 c/sec in favorable portions of an Earth orbit. The efficiency for detection of X-rays is such that with the Crab Nebula and Pulsar at the center of the 42 min field of view (FWHM) the counting rate is 1350 c/sec.

The MPC detector electronics are configured to accumulate an eight channel pulse height spectrum every 2.56 sec. In addition a time interval processor (TIP), measures the time between events (independent of energy over the 1.5 to 22 keV band), with a time resolution of a few microseconds. To accomplish the latter, an on-board memory serves as a buffer between the TIP and the telemetry system. As long as the counting rate is sufficiently low, the TIP is always operational. On the other hand, if the X-ray counting rate is high enough so that the memory fills entirely, the TIP becomes inactive until the memory is completely emptied by the telemetry. Except when the crystal spectrometer is in the focal plane, the counting rate which fills the memory is 33 c/sec. For counting rates above this threshold there will be gaps in the data stream which last for 2.56 sec. When the crystal spectrometer is in use, the threshold is 100 c/sec and the gaps last for 0.82 sec.

The MPS is coaligned with the X-ray telescope and takes data as a normal part of the Observatory operation. One of the specific research programs of the Observatory is to make use of the MPC data to prepare a time variability catalog of the brighter galactic and extragalactic X-ray sources. I would like to present a few of the results that have been obtained thus far in this program. Before doing this I would like to emphasize that this work is being performed in collaboration with several people at three institutions. My collaborators are listed in Table 1. I would especially like to take this opportunity to underscore the contributions of one of the unsung heroes of this program, Mr. Ross Lippman. Ross, an undergraduate at Harvard, must have, by now, developed a permanent crick in his neck from balancing a telephone while at the same time typing in changes to computer programs as we worked via long-distance late into the night.

THE TREE

The MPC, with its high time resolution (10 μsec), together with the long continuous observing time afforded by the Observatory, presents a challenging problem in the analysis of the data. In a thousand second observation, for example, there are 10^8 potentially interesting time scales corresponding to the number of statistically independent frequencies. Examination of such a data set for periodic behavior is in and of itself a major undertaking because of the computer time involved. Furthermore, searches for periodicity address only one aspect of the time variability of the X-ray sources. One of the most interesting aspects of X-ray astronomy has been the discovery of erratic time variations ranging from long time scales as in the case of the transient X-ray sources, to medium time scales as from the X-ray bursters, to subsecond variability as for example in the case of the blackhole candidates. Because of this aspect of the time variability and because of the need to minimize computer time we have developed, or more accurately refined, a technique for rapidly searching for and isolating erratic time variations. An example of the result of the application of this technique is illustrated in Figure 1 and I would like to take a few minutes to describe the procedure before discussing the observations.

The procedure is based on binning the data on an extremely fine time scale, calculating the variance with respect to the mean, and comparing the calculated variance to that expected on the basis of counting statistics. There is no guarantee that such a calculation will detect any time variability, even if present, as the binning time scale may be much too fine as compared to the time scale of any features in the data and/or the particular feature, such as an X-ray burst, may only span a small fraction of the total time and thus be lost as only a single contribution to the total variance. To try to account for the former effect one can consider rebinning the data on coarser and coarser time scales and recalculating the variance each time. To account for the latter effect one can repeat these calculations on subsections of the entire data set. Examination of the equations involved shows that if both the binning time scales and the subsection time scales are chosen to be integral powers of two of the finest time scales involved, then explicit binning of the data and calculation of the variance need only take place once for each subsection of data on the finest time scale. The remaining variances can then be calculated by algebraic manipulation.

Figure 1 is a graphical illustration of the results of this type of calculation, which we refer to as the "tree." The vertical bar (= branch) at the top of the tree represents the calculation for the data treated as a whole. The highest point is based on the variance of the entire data set binned on the finest time scale which in this example is 0.191 msec. The points below this, but still within the single vertical bar correspond to the finest time scale multiplied by two, by four, by eight, etc.,

until the number of bins is four. The two vertical bars immediately below the top of the tree represent the same calculation, but now for each half of the total data separately. Below this are the results for each 1/4, 1/8, 1/16, 1/32 of the data. The quantity plotted is the statistical significance of the departure of the measured variance from that expected from counting statistics; the darker the display the higher the statistical significance. For a steady source, the entire tree would appear as seen in the 24 rightmost branches at the bottom. In the example shown in Figure 1, however, a transient event has been detected and isolated to a particular portion of the data. In this example 1600 sec of data with 66×10^3 events were examined for time variability over time scales covering a range of 8×10^6 in 30 sec of (UNIVAC 1108) computer time.

TERZAN 2

The example discussed previously clearly demonstrates the detection and isolation of a single transient event. (Note the three dark branches at the bottom of the illustration in Figure 1.) This activity was detected during the HRI observation of the globular cluster, Terzan 2. As noted by Professor Giacconi, we were fortunate that J. Grindlay was at the HEAO control center during the two thousand seconds devoted to this particular experiment. His presence seems to guarantee that X-ray burst phenomena will be detected. This is only the second burst detected from the cluster, which now is unambiguously identified as the source of the X-rays, thanks to the HRI observations which have isolated the source to lie within 2 arc sec from the cluster center.

Figure 2 shows the entire time history of the burst in 2 sec intervals of TIP data. The previous burst from Terzan 2 was detected by the Goddard experiment on OSO-8 (Swank et al. 1977). Qualitatively the second burst from Terzan 2 is very similar to the first. A weak steady source is seen, in our case at an intensity approximately equal to the background counting rate. The flux is then observed to increase by almost a factor of 80 followed by what appears to be an exponential decay and lasting several hundred seconds.

Figure 3 is a plot of the major burst activity with the data binned on a time scale of 120 msec. This figure serves not only to illustrate more clearly the time development of the burst but also, unfortunately, to emphasize the gaps in the TIP data due to memory overflow. All the high time resolution observations of bursts from this source have been plagued with sampling problems. The OSO-8 experiment provided coverage of the source for 160 msec every 11 sec. That experiment was unable to determine the burst rise-time, setting an upper limit of 10 sec. Since the overall burst length from this source is much longer than that from other bursters, it is assumed that the burst rise-time was also long, of the order of several seconds. This is not the case. Figure 4 shows

the details of the rising portion of the burst. The next data point in time (not shown) occurs 2.56 sec later and is at the maximum counting rate we observed, 1345 c/sec. If we take this rate, after subtracting background, to correspond to the peak luminosity, then the results shown in Figure 4 indicate a rise to 70 percent of the peak in under 0.3 sec.

Figures 5 and 6 show the time evolution of the burst plotted in two second intervals. The first 14 sec appear saturated at a constant rate, but this may be misleading as they are based on only five samples each of 0.2 sec duration separated in time by 2.56 sec. As the counting rate decreases, however, the "on" time increases and the frequency of occurrence of the gaps decreases. At least three time constants characterize the falling portion of the burst. From 14 sec to about 34 sec the flux decreases exponentially with a time constant of 11.8 sec. This time scale was not identified in the OSO-8 burst but may not have been detectable given that they sampled the burst only once every 11 sec. At 24 sec after burst onset the decay follows a 32.0 sec e-folding for at least 50 sec. The final decay can be described by a time constant of 85.9 sec. Both of the latter time constants (32.0, 85.9) are similar to, but shorter than, those seen in the first burst of Terzan 2, i.e., 44.8 sec and 215.7 sec.

As stated earlier the peak detected luminosity to preburst luminosity ratio is 80. The energy in the burst is approximately 40 times greater than the peak luminosity which corresponds (very) approximately to 5×10^{36} ergs/sec at a distance of 1 kpc. The distance to Terzan 2 being approximately 7 kpc (Grindlay, 1978), this would put the flux at the Eddington limit for a two solar mass object. A spectral analysis of the data is currently in progress and the results will be presented at the Wellesley meeting of the AAS.

CYGNUS X-3

The light curve of the MPC TIP observations of Cygnus X-3 is shown as the histogram in Figure 7. These observations were performed when Cygnus X-3 was in an extremely low state. The MPC energy bandwidth extends to 20 kV and the energy spectrum was extremely hard during these observations, yet our mean counting rate was much lower than the minimum (2-6 keV) seen during the early Uhuru observations. The dots in the figure are the individual data points obtained during the 2.4 days of observation, and indicate the variability in the flux above and beyond that expected on the basis of counting statistics above. The two sigma error bars on individual data points are approximately the same size as the symbols shown.

Using the technique of the tree, we have examined the counting rate as a function of time and have discovered several interesting features.

Figure 8 shows one such feature, a fairly long flare which was observed on the falling portion of the light curve. A similar feature shown in Figure 9, but weaker, was again observed in the next 4.8 hr period of this source but somewhat earlier in phase. The energy spectrum of these features has not as yet been analyzed.

Figures 10, 11, and 12 illustrate the second type of feature observed in the data. This feature is referred to as a "sudden" transition, where the counting rate changes suddenly and significantly on the time scales to 10 to 20 sec. Two such transitions separated in time by approximately 500 sec are shown in Figure 10. Five 4.8 hr periods later, again two such transitions were observed, and are shown in Figure 11 but now separated in time by 1100 sec and at different phases in the 4.8 hr period than the first pair. Finally, as shown in Figure 12, at least one and possibly two transitions were observed in the 11th 4.8 hr cycle. The times and phases refer to the 4.8 hr period and the amplitudes of these features are summarized in Table 2. In general, there was insufficient coverage at all phases to establish whether or not these transitions were always present during the rising portion of the light curve, however, no sudden transitions were ever observed in either the peak or the falling portion of the light curve.

It should be noted at this point that although we have ruled out the possibility that these features are due to an attitude maneuver, we have not, as yet, examined enough data from other X-ray sources to conclusively eliminate the possibility that the sudden transitions are a manifestation of some type of systematic effect not associated with the X-ray source. Thus, our current efforts have concentrated on, not an interpretation of these features, but rather on understanding the Cygnus X-3 system as a whole. In this regard we have puzzled about the obvious asymmetry in the 4.8 hr light curve which is apparent not only in our data, but also in the majority of the historical light curves. The asymmetry can, clearly, be produced for a variety of reasons such as an anisotropic distribution of circumstellar material or an eccentric orbit. The smooth curve in Figure 9 is the light curve one would observe in the case where the modulation is due to absorption in a stellar wind with Cygnus X-3 in an eccentric orbit. In the calculation shown in the figure the eccentricity was 0.3, the inclination angle 24 degrees, and the longitude of periastron at 95 degrees. This calculation (which considered only a pure absorbing atmosphere) and the resulting parameters are not meant to be taken as an exact description of the Cygnus X-3 system; they indicate that the suggestion of an elliptical orbit can, at least in this simple model, lead to acceptable light curves which fit the data.

One consequence of the elliptical orbit hypothesis is that one might expect to see changes in the apparent shape of the light curve due to apsidal motion. Since no reversals in the asymmetry of the light curve have been observed in the 5.5 years since the source's discovery the

period would have to be long, at least of the order of 20 years. Such periods imply a companion to the X-ray source much more centrally condensed than a main sequence star. In addition, the companion must have a mass loss rate which can provide enough circumstellar matter to produce the observed X-ray modulation. This rules out compact companions (i.e., degenerate dwarfs or neutron stars) and makes it very likely that the companion is a highly evolved state filling its Roche Lobe.

REFERENCES

Gaillardetz, R., Bjorkholm, P., Mastronardi, R., Vanderhill, M., and Howland, D., 1978: I.E.E.E. Trans. on Nucl. Sci., NS-25,437.

Giacconi, R., Barnduardi, G., Briel, U., Epstein, A., Fabricant, D., Feigelson, E., Forman, W., Gorenstein, P., Grindlay, G., Gursky, H., Harnden, F. R., Henry, J. P., Jones, C., Kellogg, E., Koch, D., Murray, S., Schreier, E., Seward, F., Tananbaum, H., Topka, K., van Speybroeck, L., Holt, S. S., Becker, R. H., Boldt, E. A., Serlemitsos, P. J., Clark, G., Canizares, C., Markert, T., Novick, R., Helfand, D., and Long, K., 1979: Ap. 3., 230, 540.

Grindlay, J. E., 1978: Ap. J. (Letters), 224, L107.

Swank, J. H., Becker, R. H., Boldt, E. A., Holt, S. S., Pravdo, S. H., and Serlimitsos, P. J., 1977: Ap. J. (Letters), 212, L73.

TABLE 1. COLLABORATORS ON THE TIME VARIABILITY PROGRAM

NASA/George C. Marshall Space Flight Center

W. Darbro
R. Elsner (NAS/NRC)
P. Ghosh (NAS/NRC)
M. C. Weisskopf

McMaster University

P. G. Sutherland

Harvard-Smithsonian Center for Astrophysics

P. Hertz
J. E. Grindlay
G. S. Vaiana

TABLE 2. SUMMARY OF THE OBSERVATIONS OF THE SUDDEN TRANSITIONS IN CYGNUS X-3

Time of Occurrence (Day of 1978)	(sec)	4.8 hr Phase	Percent Change in Intensity
350	22329	0.253	15
350	22841	0.283	25
351	2650	0.120	15
351	3756	0.184	11
352	19359	0.097	14
352	20843	0.183	9

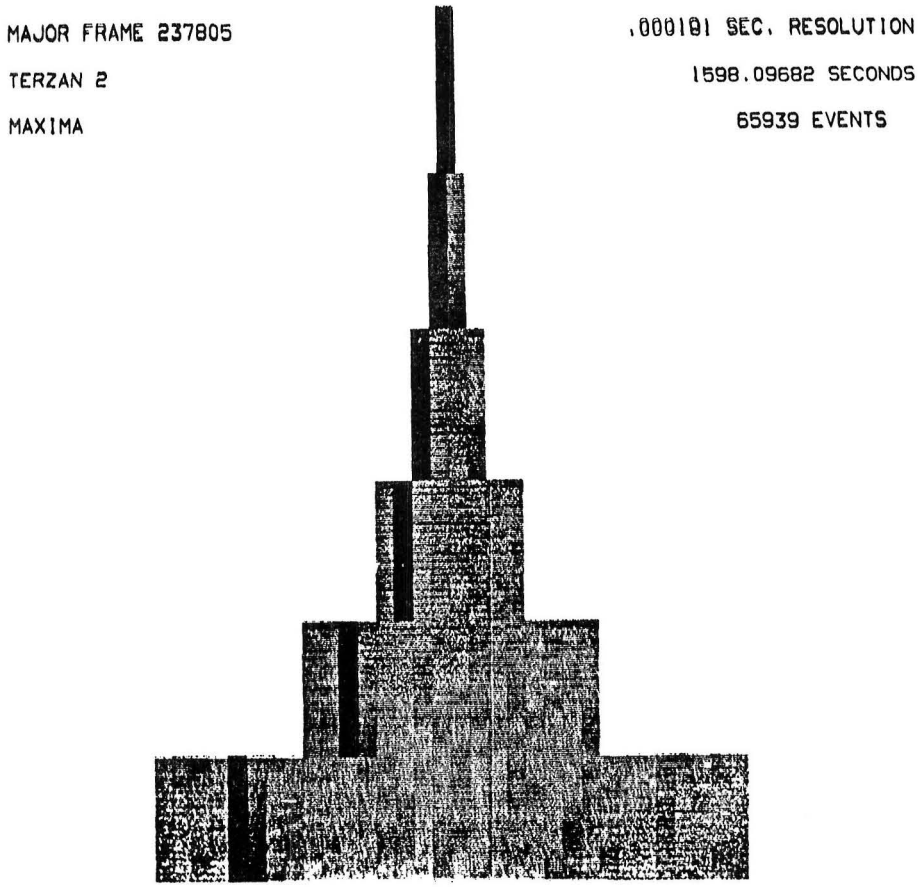

Figure 1. Graphical representation of the tree. The figure is discussed in detail in the text in Section II.

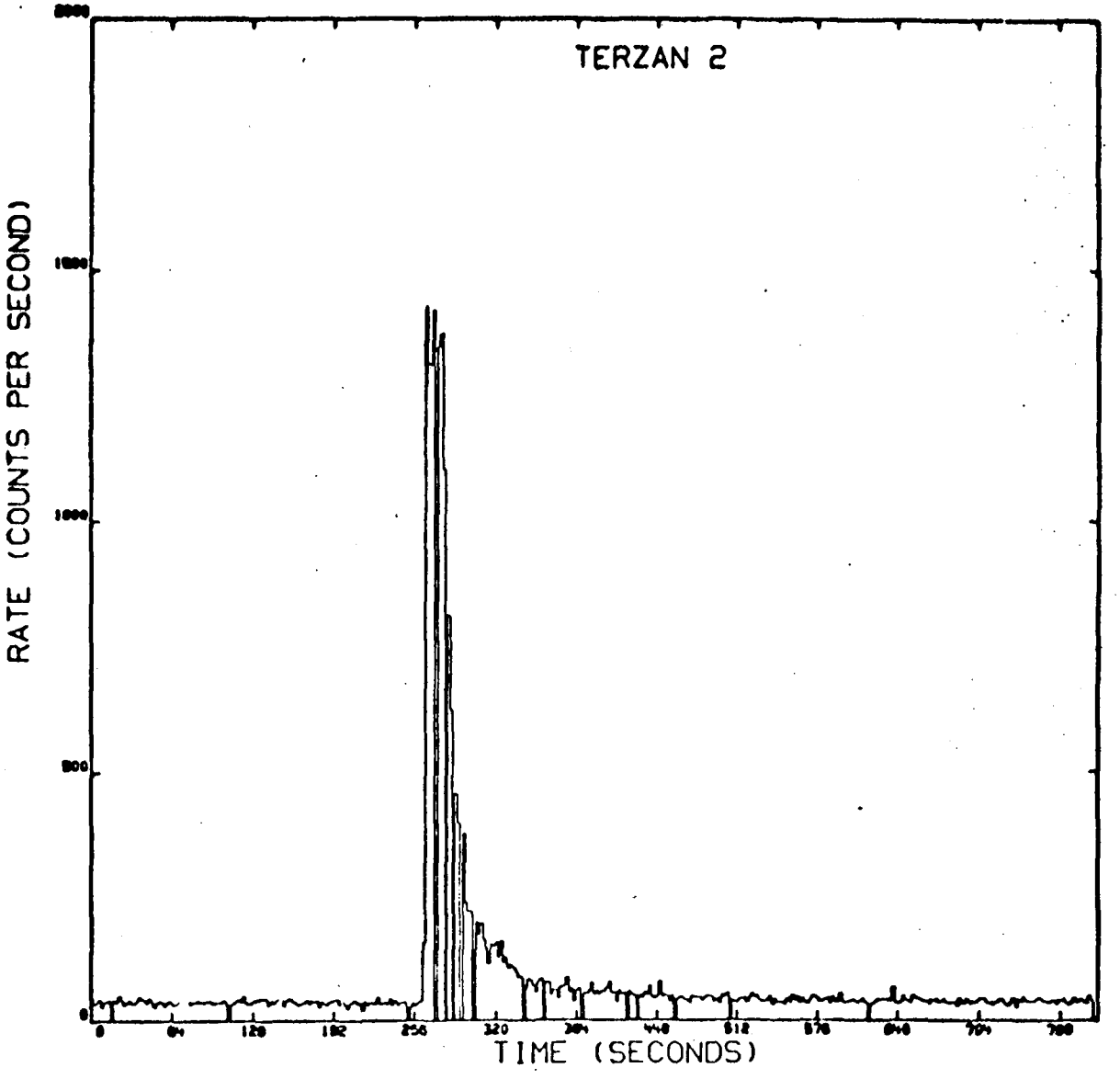

Figure 2. Counting rate versus time during the TIP observation of Terzan 2. The data are binned in 2 sec intervals.

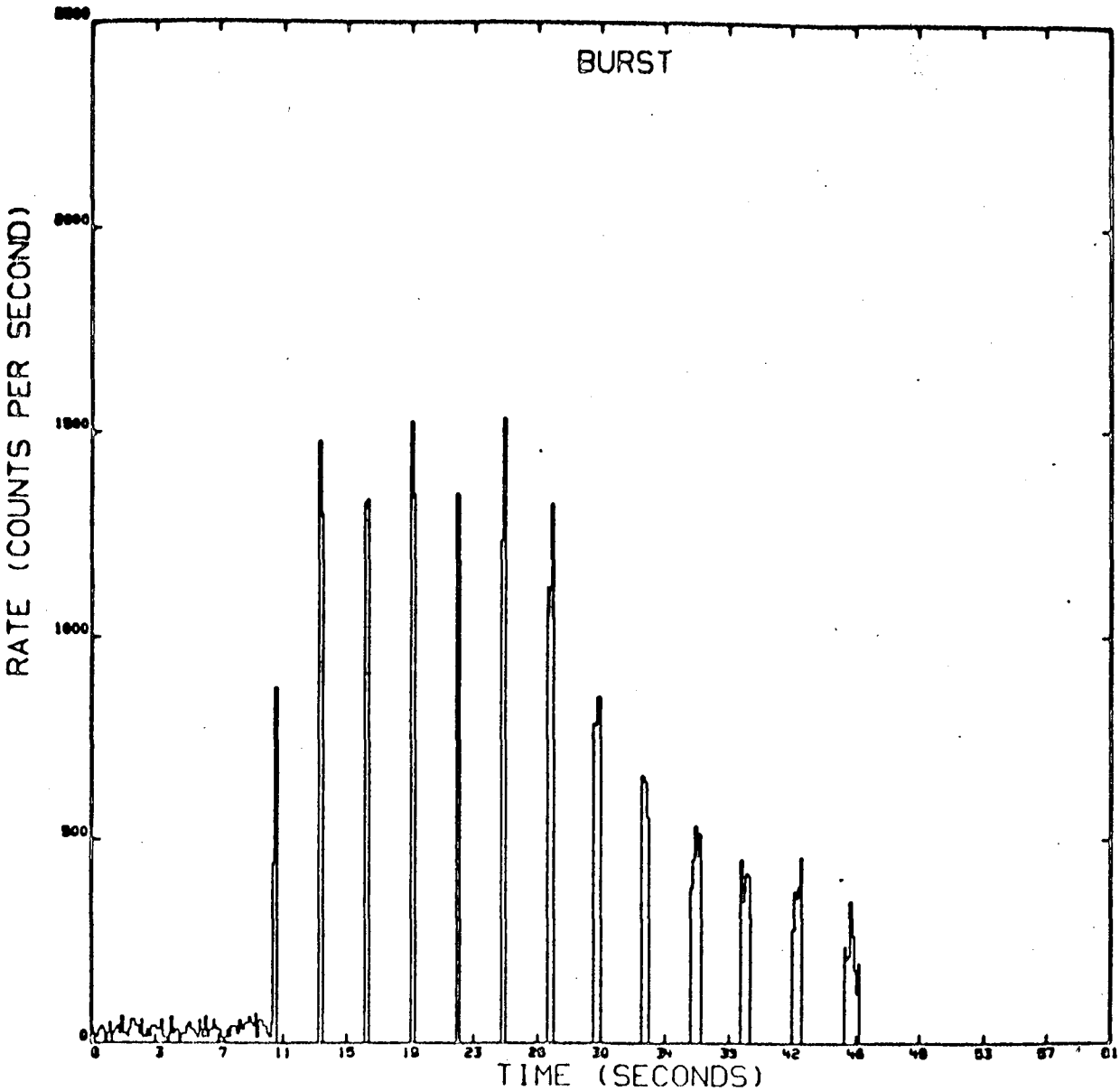

Figure 3. Forty-eight seconds of TIP data including the onset of the burst from Terzan 2. The data are binned in 0.12 sec intervals.

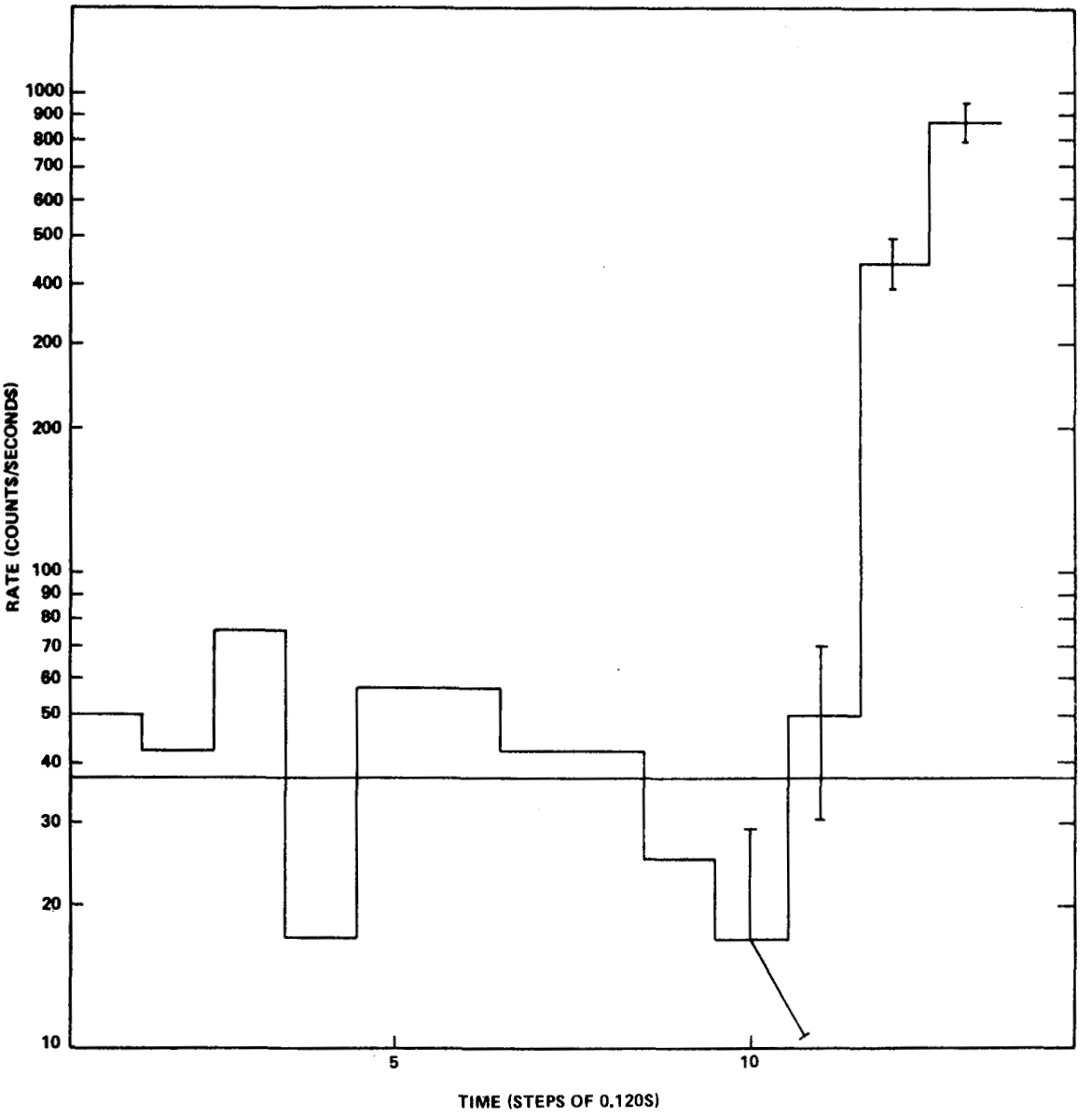

Figure 4. Burst onset. The data are binned in 0.12 sec intervals. The solid line is the mean preburst counting rate including 20 c/sec of background.

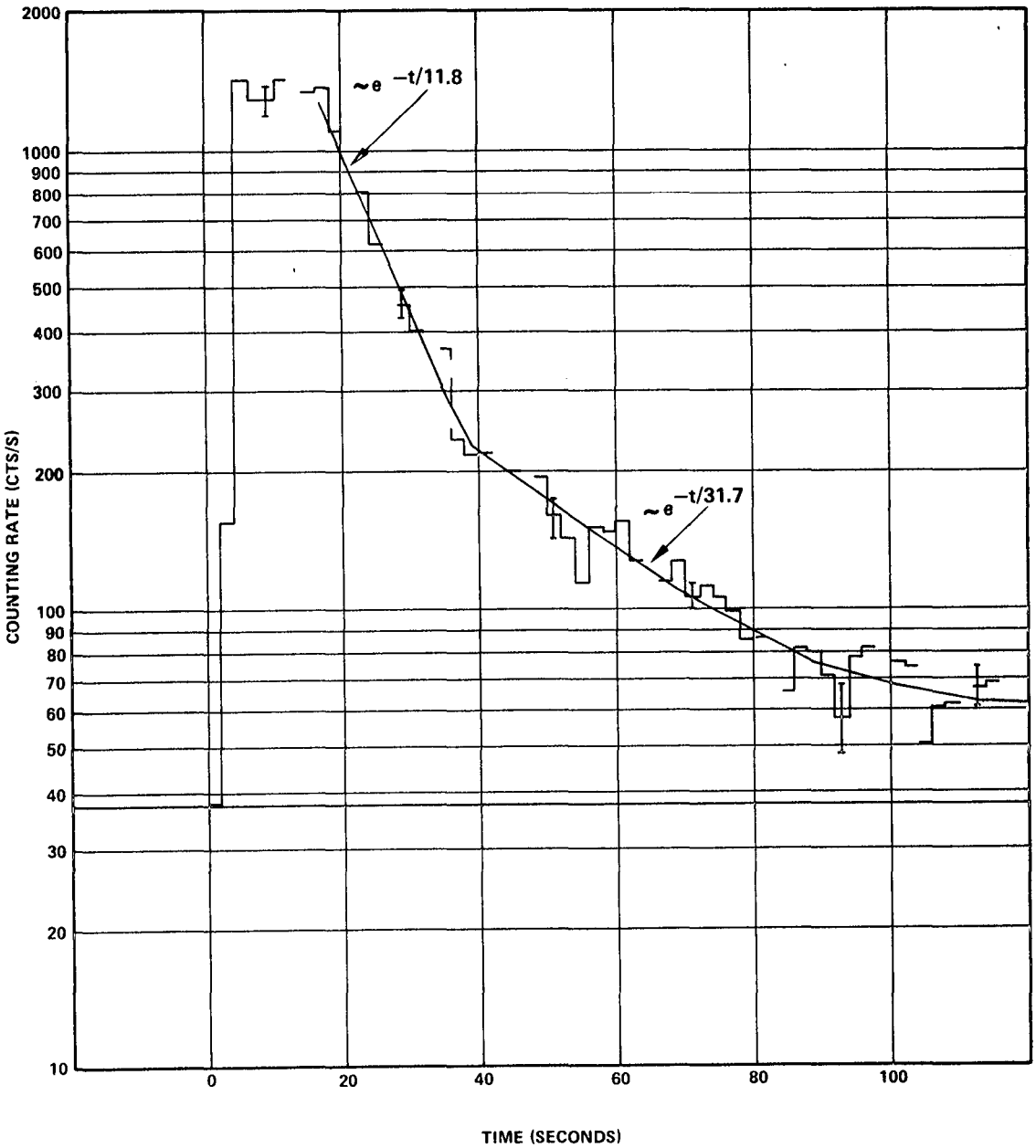

Figure 5. The time evolution of the burst from Terzan 2 plotted in 2 sec intervals. The solid line is the mean preburst counting rate including the non X-ray background.

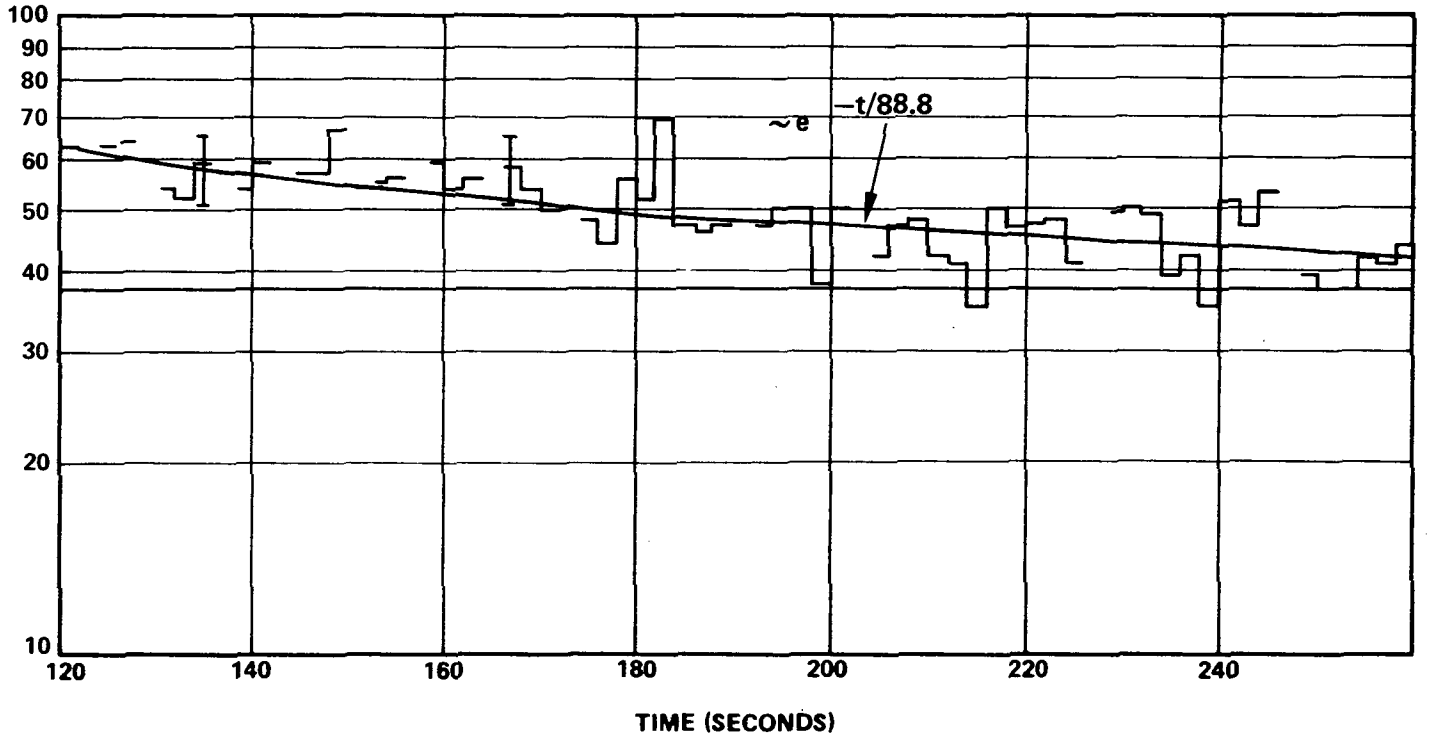

Figure 6. The time evolution of the burst from Terzan 2 plotted in 2 sec intervals. The solid line is the mean preburst counting rate including the non X-ray background.

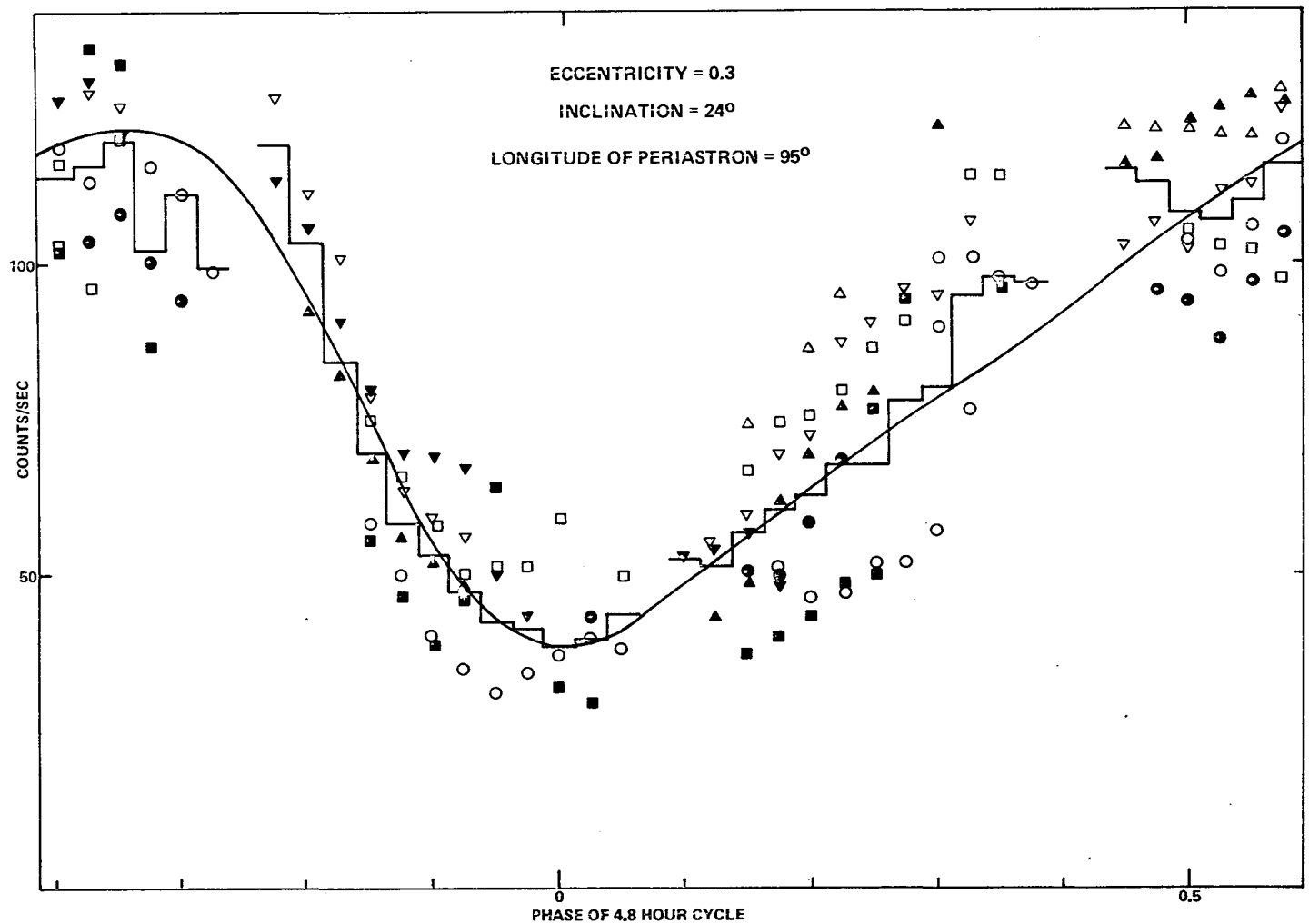

Figure 7. TIP observations of Cygnus X-3 folded modulo the 4.8 hr period. The histogram is is the mean light curve. The points are the contributions to the mean from each 4.8 hr cycle. In both cases the errors due to counting statistics are approximately the size of data points shown. These data are shown with background subtracted and corrected for aspect. The solid line is the light curve expected from a pure absorbing atmosphere produced by a stellar wind with the X-ray source in an elliptical orbit.

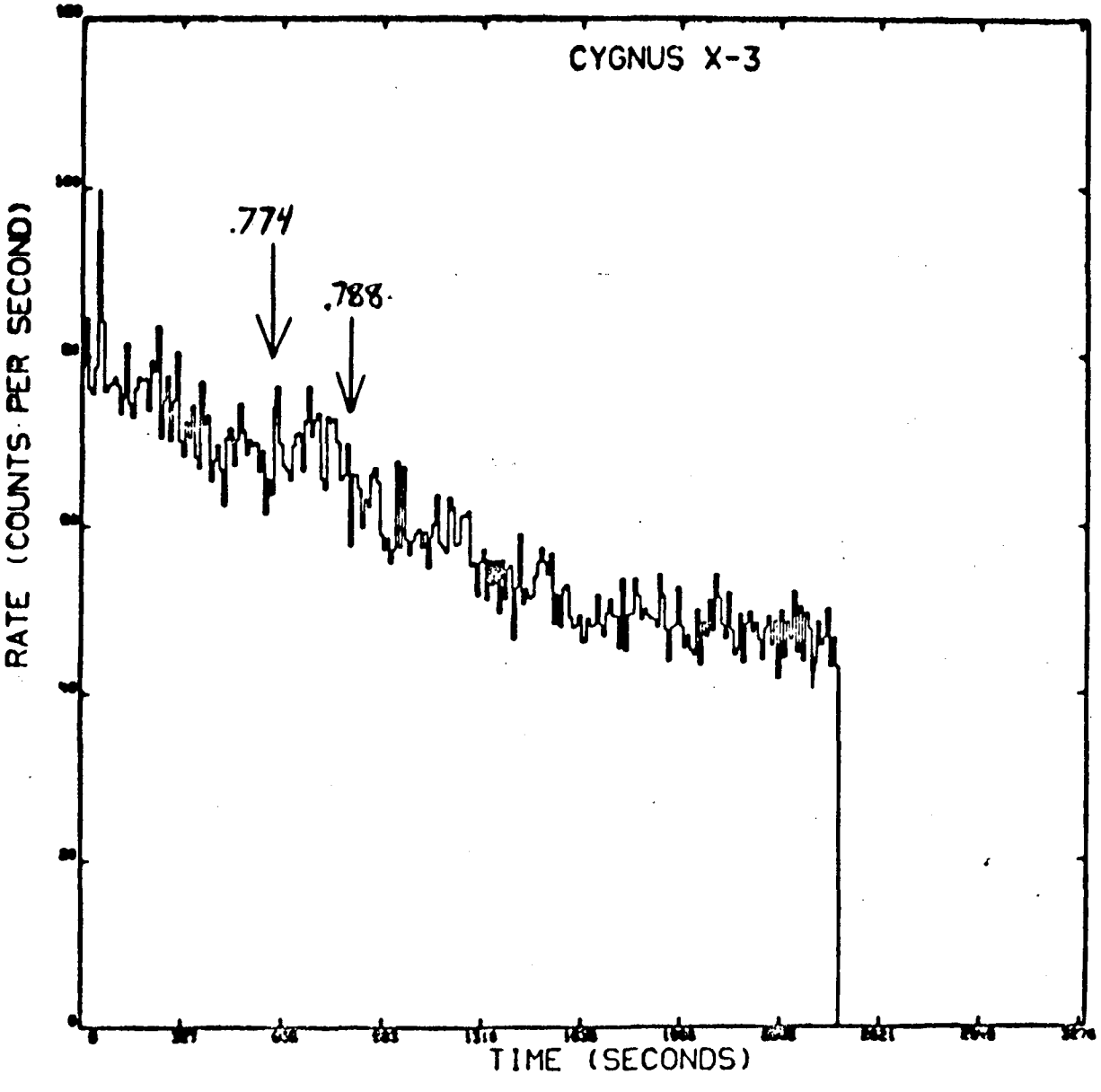

Figure 8. An X-ray flare from Cygnus X-3 detected in the falling portion of the light curve during phases 0.774 to 0.778 of the 4.8 hr period. The data are binned in intervals of 10.24 sec and are uncorrected for background and aspect.

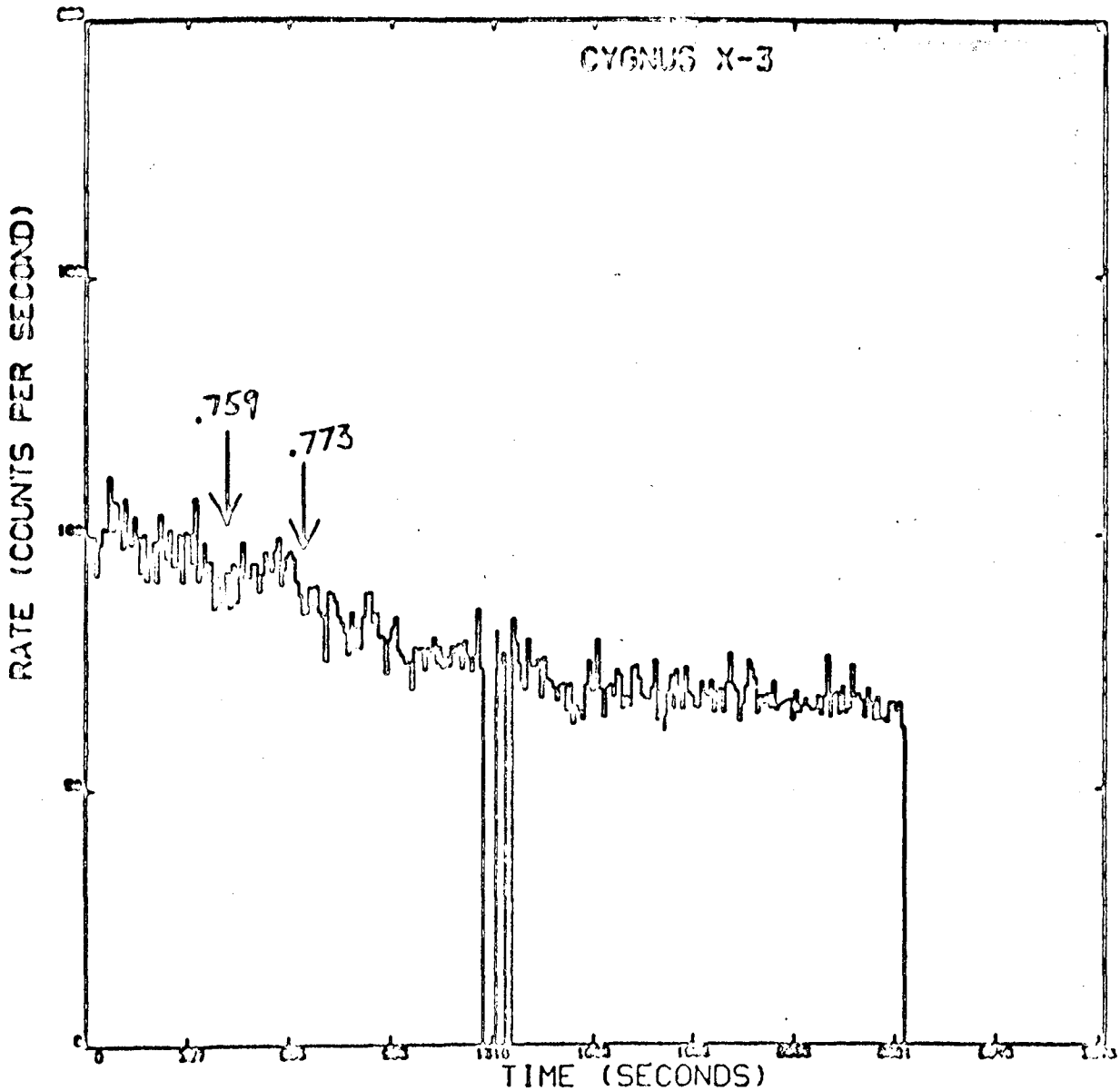

Figure 9. An X-ray flare from Cygnus X-3 detected in the falling portion of the light curve in the 4.8 hr period subsequent to the one shown in Figure 8. This could well be the same flare reappearing due to e.g. binary motion. Note that the phase of occurrence lies in the interval 0.759 to 0.773.

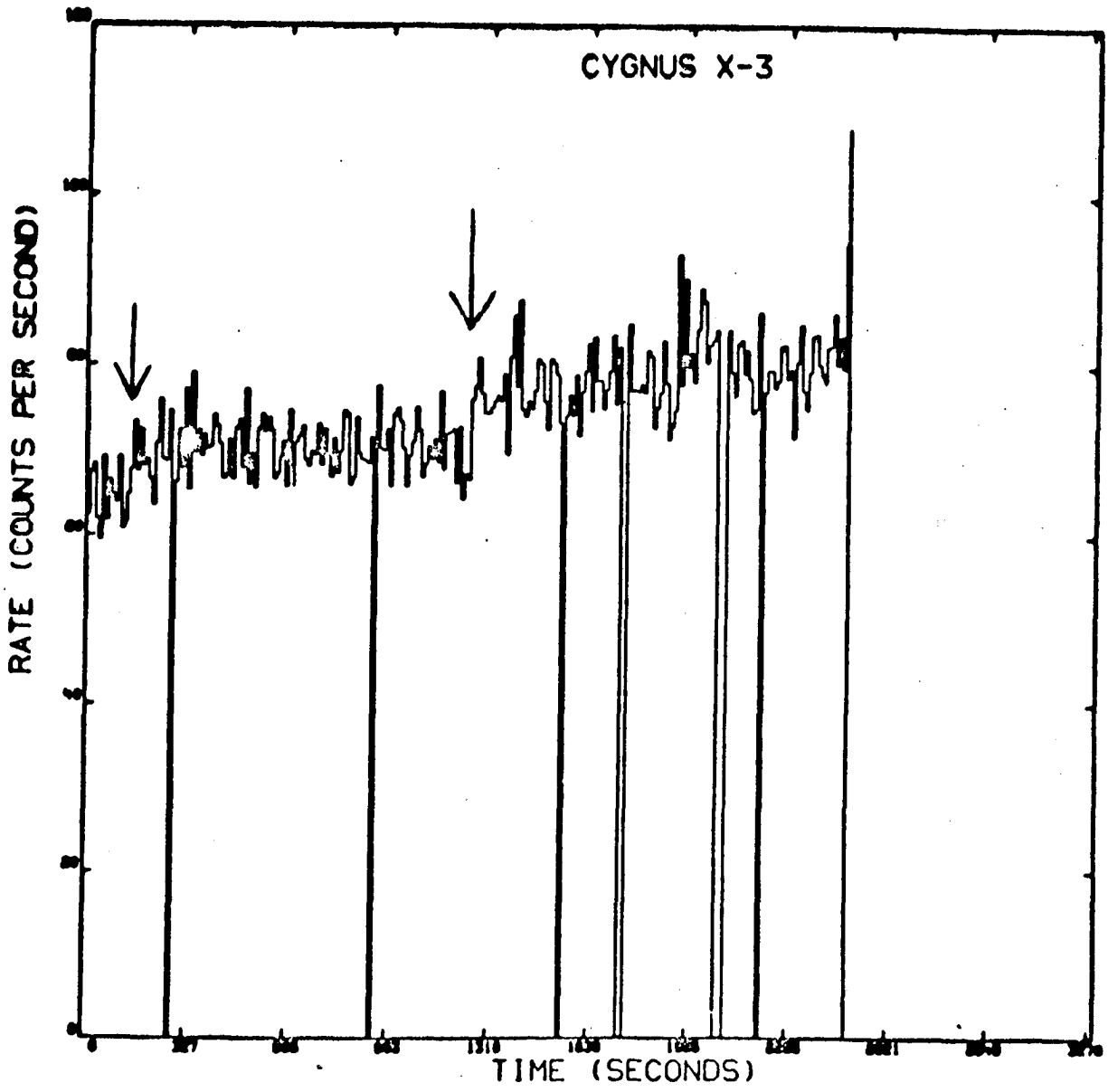

Figure 10. Sudden transition in the counting rate versus time during the TIP observations of Cygnus X-3. The data are binned in intervals of 10.24 sec and are uncorrected for background or aspect. There were no attitude maneuvers during the observations shown. The observations are summarized in Table 2 of the text.

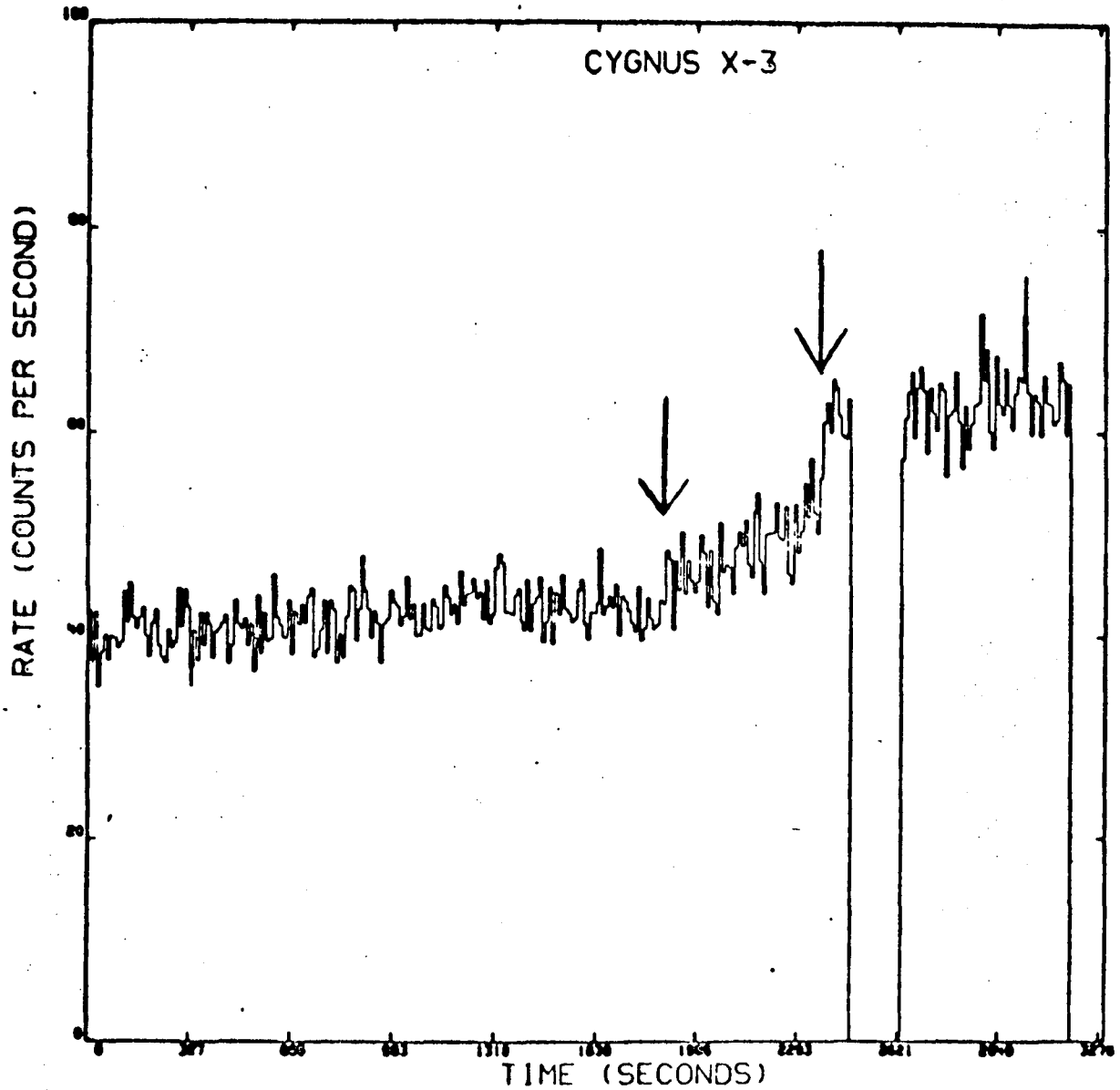

Figure 11. Sudden transition in the counting rate versus time during the TIP observations of Cygnus X-3. The data are binned in intervals of 10.24 sec and are uncorrected for background or aspect. There were no attitude maneuvers during the observations shown. The observations are summarized in Table 2 of the text.

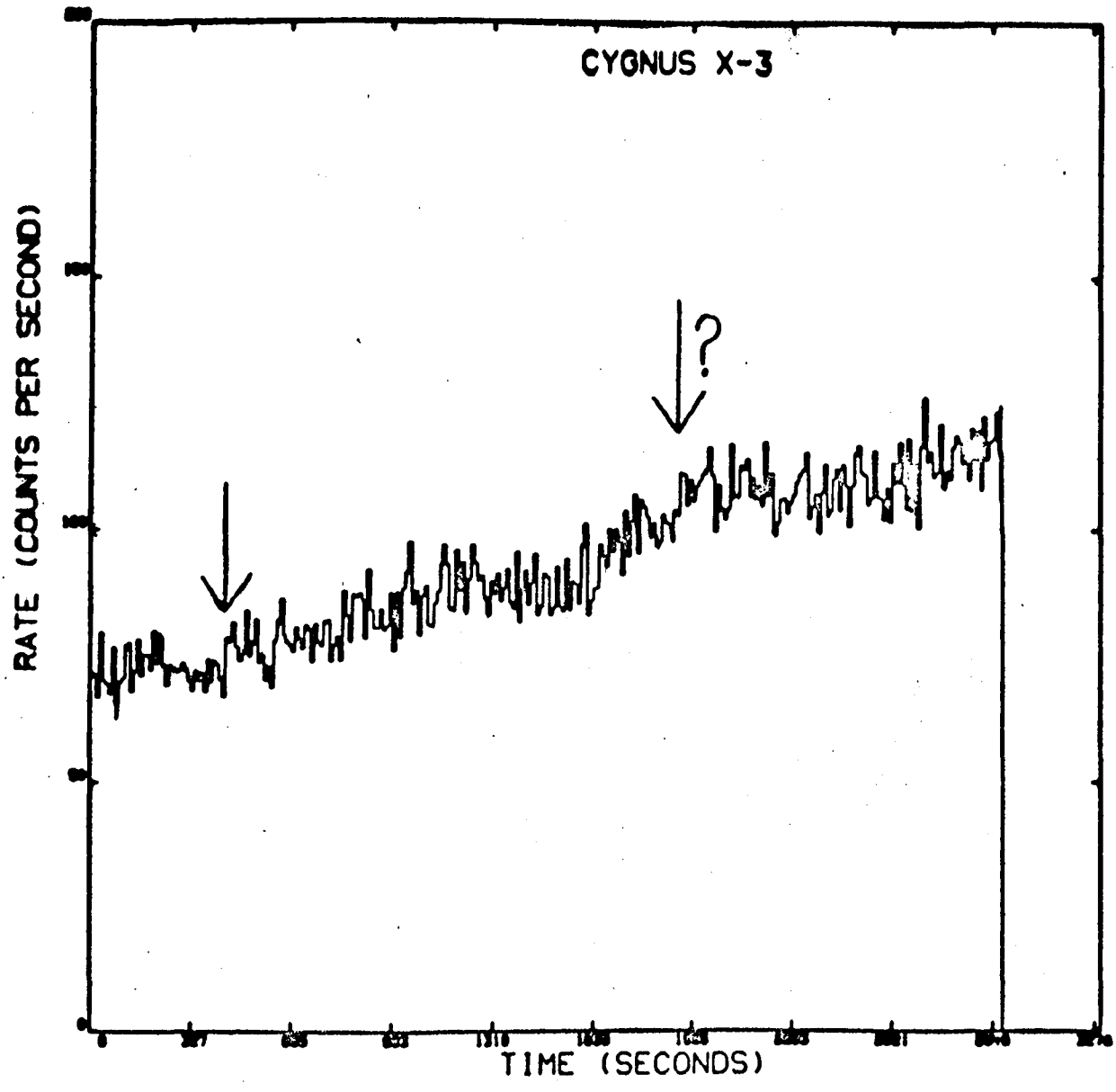

Figure 12. Sudden transition in the counting rate versus time during the TIP observations of Cygnus X-3. The data are binned in intervals of 10.24 sec and are uncorrected for background or aspect. There were no attitude maneuvers during the observations shown. The observations are summarized in Table 2 of the text.